International Journal of Nanomedicine

Dovepress
open access to scientific and medical research

Open Access Full Text Article

ORIGINAL RESEARCH

Platelet-functionalized three-dimensional poly-ε-caprolactone fibrous scaffold prepared using centrifugal spinning for delivery of growth factors

This article was published in the following Dove Press journal:
International Journal of Nanomedicine
6 January 2017
Number of times this article has been viewed

Michala Rampichová[1,2]
Matej Buzgo[1]
Andrea Míčková[1,2]
Karolína Vocetková[2]
Věra Sovková[2]
Věra Lukášová[2]
Eva Filová[2]
Franco Rustichelli[2]
Evžen Amler[1,2]

[1]Indoor Environmental Quality, University Center for Energy Efficient Buildings, Czech Technical University in Prague, Buštěhrad, [2]Laboratory of Tissue Engineering, Institute of Experimental Medicine, Czech Academy of Sciences, Prague, Czech Republic

Abstract: Bone and cartilage are tissues of a three-dimensional (3D) nature. Therefore, scaffolds for their regeneration should support cell infiltration and growth in all 3 dimensions. To fulfill such a requirement, the materials should possess large, open pores. Centrifugal spinning is a simple method for producing 3D fibrous scaffolds with large and interconnected pores. However, the process of bone regeneration is rather complex and requires additional stimulation by active molecules. In the current study, we introduced a simple composite scaffold based on platelet adhesion to poly-ε-caprolactone 3D fibers. Platelets were used as a natural source of growth factors and cytokines active in the tissue repair process. By immobilization in the fibrous scaffolds, their bioavailability was prolonged. The biological evaluation of the proposed system in the MG-63 model showed improved metabolic activity, proliferation and alkaline phosphatase activity in comparison to nonfunctionalized fibrous scaffold. In addition, the response of cells was dose dependent with improved biocompatibility with increasing platelet concentration. The results demonstrated the suitability of the system for bone tissue.

Keywords: centrifugal spinning, 3D scaffold, platelets, growth factors, cytokines, PCL

Introduction

In order to fulfill the goals of tissue engineering, scaffolding materials that support cell adhesion and proliferation are in demand. These materials should attract cells to infiltrate inside the scaffold and stimulate them to differentiate to the desired cell type. Proper cell differentiation is crucial for tissue-specific extracellular matrix (ECM) synthesis and could create newly formed fully functionalized tissue. To fulfill such expectations, tissue-engineered scaffolds are combined with drug delivery carriers and serve as a mechanical support not only for cells but also for their stimulation.

Among the wide spectrum of scaffolding materials used in tissue engineering, nanofibers and microfibers raise much attention. With diameters similar to the compounds of ECM, the fibers mimic the natural environment for cells and enhance their adhesion and proliferation.[1,2] The most commonly used technology for producing ultrafine fibers for tissue engineering applications is electrospinning. To overcome electrospinning limitations, such as low production capacity and sheet structure with limited layer thickness, alternative methods such as melt-blown and centrifugal spinning have been used.[3]

Centrifugal spinning (Forcespinning™) is a technology that uses centrifugal force to produce ultrafine fibers from melts and solutions.[4] The polymeric solution or melt is placed in a rotating chamber with a thin orifice. The applied centrifugal speed has to be strong enough to overcome surface tension of the solution. The polymer solution is ejected from the orifice,

Correspondence: Michala Rampichová
Indoor Environmental Quality, University Center for Energy Efficient Buildings, Czech Technical University in Prague, Trinecka 1024, 273 43, Buštěhrad, Czech Republic
Tel/fax +420 296 442 387
Email michala.rampichova@cvut.cz

submit your manuscript | www.dovepress.com
Dovepress
http://dx.doi.org/10.2147/IJN.S120206

and emerged jets are stretched and deposited on a collector. The Forcespinning technology has been used for fabricating tissue engineering scaffolds from various polymers, such as poly-ε-caprolactone (PCL),[4–6] gelatin,[5] poly(L-lactic acid) (PLLA),[7] and poly-lactic-co-glycolic acid (PLGA).[8] Loordhuswamy et al[5] used in their study PCL in combination with gelatin to produce fibrous meshes and tested them in vitro and in vivo for wound healing. Zander[4] used a rotating collector to deposit aligned PCL fibers and used them to culture neuronal PC12 cells. It was shown that the cells extended their neurites along the fibers.

However, the structure of the scaffold alone is often not sufficient to promote tissue healing. In order to simulate the physiological gradients of signaling molecules regulating cellular fate, the scaffolds are often combined with drug delivery systems. Platelets are frequently used in tissue engineering and regenerative medicine as a source of natural cytokines and growth factors. Platelets play an important role in wound healing and regeneration and inflammatory response. Alfa granules of platelets contain a wide range of growth factors, including PDGF, TGF-β, PDAF, VEGF, EGF, PDEGF, ECGF and IGF.[9] It has been reported that the use of platelets is beneficial for healing of bone,[10] cartilage,[11] tendon,[12] hernia[13] and skin[14] defects. One of the main advantages of using platelets as a source of growth factor is the possibility of autologous use, which reduces the immune reaction.

In our previous experiment, platelets were used to make electrospun PCL nanofibers functional.[11] Platelets adhered effectively to nanofibers, and the released growth factors enhanced the adhesion and proliferation of chondrocytes. The system of electrospun PCL nanofibers with adhered platelets was also tested in a study by Plencner et al.[13] The nanofibrous samples with adhered platelets were tested with fibroblast as a potential chirurgical mesh. The study showed that the platelets improved the properties of PCL nanofibers. In a study by Diaz-Gomez et al,[15] PCL nanofibers prepared using electrospinning were soaked in platelet-rich plasma (PRP) and subsequently lyophilized. It was shown that growth factors were released from the scaffold-enhanced adhesion and proliferation of mesenchymal stem cells (MSCs). No effect of MSC differentiation was detected.

In the current study, PCL three-dimensional (3D) fibrous meshes prepared via centrifugal spinning (Forcespinning) were combined with adhered platelets. The adhered platelets were used as a natural source of cytokines and growth factors for stimulating cell adhesion, proliferation and osteogenic differentiation. The fibers prepared using centrifugal spinning were expected to possess the same adhesive capacity as electrospun fibers, with the advantage of a 3D mesh structure. A 3D structure is essential for bone tissue engineering.

Materials and methods

Fibrous scaffold preparation using centrifugal spinning technology

Fibrous meshes were prepared using a centrifugal spinning device (Cyclone 1000 L/M Forcespinning® device; FibeRio, McAllen, TX, USA). PCL (Sigma-Aldrich, St Louis, MO, USA) was dissolved in a mixture of chloroform and ethanol in a volume ratio of 9:1 to make 40% solution. An orifice G30 at a rotation speed of 6,000× *g* was used to prepare the fibrous meshes. Fibers were deposited on spunbond textile using vacuum-assisted deposition.

Characterization of fibrous scaffolds prepared using centrifugal spinning

The prepared fibers were visualized using a scanning electron microscope (SEM), and fiber diameter was determined. Samples were coated with a thin layer of platinum using a Quorum Q 150R S device (3 cycles; Quorum Technologies, Lewes, UK) and visualized using SEM (Vega 3; Tescan, Brno, Czech Republic). The acceleration voltage for all samples was 10 kV. Fiber diameter and pore size were analyzed in the ImageJ program.

Adhesion of platelets on fibrous scaffolds

Leukocyte-depleted platelets derived from buffy coat in additive solution were purchased from the Transfusion Station at Šumperk hospital. The bag contained platelets from 4 donors. According to the Czech legislation of blood transfusion, blood products not used for therapy can be used for scientific purposes. Therefore, approval from an ethics committee was not necessary for this study. All donors signed an informed consent, agreeing to the use of their blood for scientific purposes. Platelets were centrifuged at 120× *g* for 7 min for sedimentation and removal of residual erythrocytes. Subsequently, the supernatant was transferred into a new tube and centrifuged (2,200× *g*; 10 min) to retrieve the pellet of platelets, which was resuspended in Platelet Additive Solution SSP+ (Macopharma, Tourcoing, France). Platelets were then diluted to required concentrations in SSP solution: $3{,}000\times10^9$/L (corresponds to 10× concentrated physiological concentration (PC); P1), 900×10^9/L (corresponds to 3× concentrated PC; P2), 300×10^9/L (corresponds to PC; P3), 100×10^9/L (3× diluted PC; P4) and 30×10^9/L (10× diluted PC; P5).

Quantification of selected growth factors released from platelets

To quantify the concentrations of pro- and anti-inflammatory cytokines and growth factors, a Bio-Plex 200 Multiplex

System (Bio-Rad Laboratories, Hercules, CA, USA) and enzyme-linked immunosorbent assay (ELISA, DuoSet®; R&D Systems, Minneapolis, MN, USA) were used. Platelet lysate was prepared by the freeze/thaw method. Platelets at a concentration of 900×10^9/L were lysed using 3 freeze/thaw cycles (−80°C and 37°C) and subsequently centrifuged at 3,422× *g* for 10 min to remove the cell membranes. To analyze the cytokine content of the platelet lysate, the commercially available cytokine panel (Bio-Plex ProTM Human Cytokine 27-plex Assay; Bio-Rad Laboratories) was used in accordance with the manufacturer's instructions. The assay allows multiple cytokines to be quantified simultaneously in 1 well. Briefly, the platelet lysate was incubated with a set of color-coded magnetic beads, each conjugated with an antibody directed against a specific mediator. Biotinylated detection antibody was added and allowed to bind to streptavidin–phycoerythrin. To remove the unbound protein, thorough washing series were performed in between each step by an automatic wash station (Bio-Plex ProTM II). Finally, the data were analyzed using a BioPlex 200 instrument fitted with BioManager analysis software (5-parameter curve fitting).

To observe the distribution of growth factors released from platelets, a sandwich ELISA was used. SDF-1α and bFGF were determined according to the guidelines (Peprotech, Rocky Hill, NJ, USA). P-Selectin, EGF, HGF, KGF, IGF-1, TGF-β, thrombospondin and VEGF were quantified according to the manufacturer's instructions (DuoSet).

Release of thrombospondin from platelets adhered on fibers

Thrombospondin was used as a model molecule to determine the release profile of growth factors from the platelet-functionalized samples. Scaffolds of 11 mm diameter were punched out of the prepared fibrous samples. The scaffolds were functionalized with different concentrations of platelets and incubated in phosphate-buffered saline (PBS; 500 µL) at 37°C. At given time points, the PBS was collected, replaced with a fresh one and the samples were stored at −20°C until analysis. To quantify the released thrombospondin, ELISA was conducted according to the manufacturer's instructions (DuoSet).

Release of proteins from platelets adhered on fibers

Overall protein quantification was used to analyze the kinetics of growth factor release from platelets. Scaffolds of 11 mm diameter were punched out of the prepared fibrous samples. The scaffolds were functionalized with different concentrations of platelets and incubated in PBS (500 µL) at 37°C. At given time points, the PBS was collected, replaced with a fresh one and the samples were stored at −20°C until analysis. To quantify the released protein, the QuantIT Protein assay (Life Technologies, Carlsbad, CA, USA) was used according to the manufacturer's instructions. Briefly, 10 µL of the sample was mixed with 200 µL of fluorescent probe. The fluorescence intensity was measured using a multimode reader (Synergy H1; Biotek, Winooski, VT, USA) at excitation wavelength (λ_{ex}) =470 nm and emission wavelength (λ_{em}) =570 nm. Samples were analyzed in 4 independent measurements.

Cell seeding of the scaffold and adhesion of platelets

Before cell seeding, PCL nanofibers were cut into round patches of 6 mm diameter and sterilized using ethylene oxide. Samples were seeded with 10×10^3 MG-63 cells (Cell Lines Service GmbH, Eppelheim, Germany) per well of a 96-well plate. Cells adhered to the scaffolds for 2 h in 30 µL of culture medium (Dulbecco's Modified Eagle's Medium [DMEM] supplemented with 2% fetal bovine serum and penicillin/streptomycin; Sigma-Aldrich). Subsequently, 20 µL of platelet suspensions in different concentrations (P1–P5 as mentioned earlier) were added and left to adhere for another hour. Finally, 250 µL of culture medium was added. Culture medium was not changed during the experiment. Six different samples were prepared. Five groups with different concentrations of platelets adhered on fibrous scaffolds (PCL/P1–P5), and fibrous scaffold without any platelets as a control (PCL). Scaffolds with adhered platelets in different concentrations (P1–P5) without cells were used as a control. The results acquired from these samples were used as a control of the interaction of platelets with the used methods and were deducted from the values measured on the cell-seeded samples.

Cell viability analysis

The metabolic activity of cells was measured using an MTS assay (CellTiter 96® AQueous One Solution Cell Proliferation Assay; Promega, Madison, WI, USA). Twenty microliters of MTS solution were added to 100 µL of the sample medium and incubated for 2 h at 37°C. Subsequently, 100 µL of the cultured solution was transferred to a new clean well. The absorbance of the medium was detected using spectrophotometry at 490 nm (reference wavelength: 690 nm).

Cell proliferation analysis

The proliferation of chondrocytes on the scaffold was determined from the amount of DNA (Quant-iT™ dsDNA

Assay Kit; Life Technologies). The proliferation of chondrocytes on scaffolds was tested on days 1, 3, 7 and 14. The scaffolds were put into a vial with 200 µL of cell lysis solution (0.2% v/v Triton X-100, 10 mM Tris [pH 7.0] and 1 mM EDTA) and processed through 3 freeze/thaw cycles; the scaffold was first frozen at −70°C and thawed at room temperature. Between each freeze/thaw cycle, the scaffolds were roughly vortexed. A sample (10 µL) was mixed with 200 µL of reagent solution, and fluorescence intensity was detected using a multiplate fluorescence reader (Synergy HT; Winooski, VT, USA; λ_{ex} =485 nm and λ_{em} =525 nm). The DNA content was determined according to the calibration curve using the standards in the kit.

Visualization of cell adhesion and proliferation on scaffolds

3,3′-Diethyloxacarbocyanine iodide, DiOC6(3), staining was used to detect cell adhesion on the scaffolds on days 1, 7 and 14 (Molecular Probes, Eugene, OR, USA). The samples were fixed with frozen methyl alcohol (−20°C) for 10 min. Fluorescent probe DiOC6(3) (1 µg/mL in PBS, pH 7.4; Thermo Fisher Scientific, Waltham, MA, USA) was added and incubated with the samples for 45 min at room temperature. Subsequently, the samples were rinsed with PBS, and propidium iodide (PI; 5 µg/mL in PBS; Sigma-Aldrich) was added for 10 min, followed by rinsing with PBS. The samples were visualized using a ZEISS LSM 5 DUO confocal microscope (PI: λ_{ex} =561 nm, λ_{em} =630–700 nm and DiOC6(3): λ_{ex} =488 nm, λ_{em} =505–550 nm).

Detection of alkaline phosphatase (ALP) activity

ALP activity was measured using a 1-Step™ PNPP kit (Thermo Fisher Scientific). A total of 100 µL of p-nitrophenyl phosphate (PNPP) was added to each well and incubated for 30 min. Subsequently, the reaction was stopped with 2N NaOH. Absorbance was measured using a spectrophotometer at 405 nm (Synergy HT).

Detection of osteogenic marker using indirect immunofluorescence staining

The presence of osteocalcin (OCN), a marker typical for osteogenic differentiation, was confirmed using indirect immunofluorescence staining on days 1, 7 and 14. Samples were fixed with 4% formaldehyde for 10 min, washed with PBS and incubated in 3% fetal bovine serum (FBS) in PBS/0.1% Triton for 30 min at room temperature. Primary monoclonal antibody against OCN (OCG3; Abcam, Cambridge, UK; dilution 1:20) was added, and the samples were incubated overnight at 2°C–8°C. After 3 washes with PBS/0.05% Tween, the samples were incubated with secondary antibody, Alexa Fluor 488-conjugated antimouse antibody, for 45 min. Subsequently, a solution of PI was added for 10 min (5 µg/mL in PBS) to visualize the cellular nuclei. Finally, the samples were washed 3 times with PBS/0.05% Tween. A confocal microscope (ZEISS LSM 5 DUO) was used to detect the present OCN (Alexa Fluor 488: λ_{ex}=488 nm, λ_{em} =505–550 nm and PI: λ_{ex} =561 nm, λ_{em} =630–700 nm).

Statistical analysis

Quantitative data are presented as mean values ± standard deviation (SD). The averaged values were determined from at least 3 independently prepared samples. Results were evaluated statistically using one-way analysis of variance and Student–Newman–Keuls test (SigmaStat 12.0; Systat, San Jose, CA, USA).

Results

Characterization of the prepared scaffolds

Six different scaffold types were prepared. Fibrous meshes were combined with 5 different concentrations of platelets: maximum concentration of platelets (3,000×10^9 platelets/L; PCL/P1), 3× diluted concentration of platelets (PCL/P2), 10× diluted concentration of platelets (PCL/P3), 30× diluted concentration of platelets (PCL/P4) and 100× diluted concentration of platelets (PCL/P5). Plain PCL fibers were used as a control.

PCL fibers were prepared successfully and showed nano/microfibrous morphology. The mean diameter of microfibers was ~1,380±427 nm. The mean diameter of the dominant nanofibrous fraction was 504±148 nm. The mean pore size was 7.11±11.9 µm^2, and 20% of pores were bigger than 10 µm^2. In addition, from the micrograph it is apparent that platelets successfully adhered to the PCL samples (Figure 1). Platelets were partially activated and formed a fibrin network on the scaffolds. Platelets were visible on the scaffolds even after 14 days of the experiment (Figure 1B). The mean diameter of platelets on day 1 was 1,080±178 nm and on day 14 was 2,465±370 nm.

Growth factors content in platelets and their release

Platelets used in the experiment were analyzed using a multiplexed protein assay (X-MAP assay; BioPlex, Bio-Rad, Hercules, CA, USA), and the content of cytokines, chemokines and growth factors was evaluated (Table 1). The analysis showed a higher presence of pro-inflammatory cytokines compared to

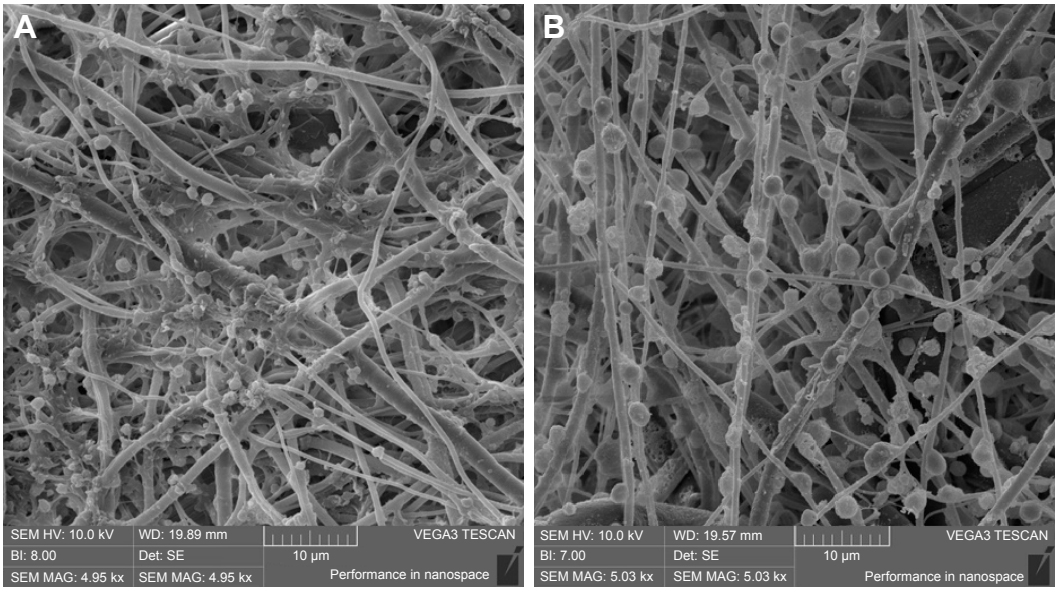

Figure 1 SEM visualization of platelet adhesion on PCL fibers.
Notes: Platelets were partially activated and formed a fibrin net 24 h after adhesion (**A**). Platelets were visibly adhered on fibers even after 14 days of the experiment (**B**).
Abbreviations: SEM, scanning electron microscope; PCL, poly-ε-caprolactone.

anti-inflammatory cytokines such as IL-1ra (340±4 pg/mL) and IL-10 (109±7 pg/mL). The IL-4 and IL-13 were detected in concentrations <50 pg/mL. The pro-inflammatory cytokines were present in higher concentration: IL-17 (1,774±10 pg/mL), IL-8 (133±30 pg/mL), IL-9 (139±12 pg/mL), IL-15 (108±6 pg/mL), INF-γ (299±11 pg/mL) and TNF-α (204±9 pg/mL). The concentrations of IL-1b, IL-2, IL-5, IL-6 and IL-7 were <50 pg/mL. RANTES was the dominant chemokine present in platelets (14,721±239 pg/mL). In addition, MIP-1b (176±68 pg/mL), eotaxin (122±8 pg/mL), IP-10 (383±22 pg/mL) and MCP-1 (113±7 pg/mL) were present in concentrations >100 pg/mL. However, from the tissue engineering point of view, the growth factors have the highest importance in stimulating cell proliferation and differentiation. PDGF-bb was the most abundant growth factor identified by X-MAP assay (9,218±313 pg/mL). VEGF (750±24 pg/mL) and bFGF (379±10 pg/mL) were present in higher concentrations. G-CSF and GM-CSF were also present in concentrations >100 pg/mL. In addition, ELISA was performed for quantification of additional growth factors. TGF-β (76,817±6,384 pg/mL), EGF (403±32 pg/mL) and HGF (530±16 pg/mL) had the highest concentration. In addition, ELISA confirmed a high concentration of thrombospondin as an antiangionetic factor (94,200±10,575 pg/mL) and P-selectin (4,667±80 pg/mL) as a marker of alpha-granule release.

To visualize the release kinetic of growth factors (GFs) from the platelets adhered on fibers, thrombospondin was used as a model protein. Thrombospondin is an inhibitor of neovascularization, which is contained in platelets at high concentrations. The thrombospondin concentration was detected in samples collected at selected time points, and its cumulative release was evaluated. The concentration of thrombospondin in the samples collected from the PCL/P4 (30× diluted maximum platelet concentration) and PCL/P5 (100× diluted maximum platelet concentration) scaffolds was below the limit of detection of the thrombospondin ELISA kit, therefore only the acquired data from the PCL/P1 (maximum platelet concentration), PCL/P2 (3× diluted maximum platelet concentration) and PCL/P3 (10× diluted maximum platelet concentration) are listed in the graph (Figure 2A). As is visible from Figure 2A, thrombospondin was released through the first 7 days of the experiment from the PCL/P1 sample (the highest concentration of adhered platelets). With decreasing concentration of the adhered platelets, the plateau phase was reached earlier in the experiment (day 3 for the PCL/P2 sample and day 1 for the PCL/P3 sample).

Besides thrombospondin release, the overall protein was measured by sensitive fluorescence probe (Figure 2B). The overall protein release overcomes the detection limit of ELISA, as all proteins released from platelets are measured in a single reaction. In addition, the detection limit of the fluorometric assay is improved compared to colorimetric determination. Therefore, the release pattern from all samples was measurable. The results are in accordance with ELISA. The amount of released proteins showed dose-dependent release in higher concentrations (10× PC, 3× PC). In this case, the release time was prolonged compared to lower platelet concentrations. On the other hand, in less

Table 1 Growth factors content in platelets measured using multiplexed protein assay and ELISA

Mediator	Concentration (pg/mL)	SD
Anti-inflammatory cytokines		
IL-1ra	340	4
IL-4	168	15
IL-10	109	7
IL-13	13	4
Pro-inflammatory cytokines		
IL-1b	12	6
IL-2	33	5
IL-5	29	6
IL-6	31	9
IL-7	53	6
IL-8	134	30
IL-9	139	12
IL-12 (p70)	229	4
IL-15	108	6
IL-17	1,774	10
IFN-γ	299	11
TNF-α	204	9
Chemokines		
RANTES	14,722	239
MIP-1a	25	4
MIP-1b	177	68
Eotaxin	122	8
IP-10	383	22
MCP-1 (MCAF)	114	7
Growth factors		
VEGF	750	24
PDGF-bb	9,218	313
FGF basic	379	10
G-CSF	219	1
GM-CSF	164	6
Growth factors measured using ELISA		
KGF	128	11
EGF	403	32
HGF	530	16
IGF-1	283	20
TGFb1	76,817	6,384
SDF-1α	67	27
Thrombospondin	94,200	10,575
P-Selectin	4,667	80

Abbreviations: ELISA, enzyme-linked immunosorbent assay; SD, standard deviation.

concentrated samples, results were influenced by proteins obtained in plasma, which were comparable in all samples. Concentrations of plasma proteins were so high compared to proteins contained in platelets that differences between samples were minimal.

Cell metabolic activity and proliferation on scaffolds

Cell metabolic activity and cell proliferation on scaffolds were examined using MTS test and DNA amount analysis on days 1, 3, 7, 10 and 14 (Figure 3). Cell adhesion was similar on all the scaffolds 24 h after seeding (Figure 3A). Cells started to proliferate faster on samples with higher platelet concentrations. The most visible proliferation was on scaffolds with the largest number of platelets (PCL/P1 and PCL/P2) on day 3. Cells continuously proliferated until day 7, where the highest number of cells was detected on PCL/P1. Lower proliferation was shown on PCL/P2 and PCL/P3 and the lowest on PCL/P4, PCL/P5 and PCL. Although the cell numbers started to decrease in PCL/P1, PCL/P2 and PCL/P3 samples from day 7, the highest number of cells was still detected in the PCL/P1 on days 10 and 14. No statistical difference was seen between the other groups.

The metabolic activity of the cells was highest in the sample with the most concentrated platelets (PCL/P1) as early as 1 day after the seeding (Figure 3B). The metabolic activity continuously increased and was highest in the PCL/P1 and PCL/P2 samples on days 10 and 14. On the other hand, relating the metabolic activity to the DNA content offered a different point of view (Figure 3C). The highest metabolic activity was seen in PCL/P1 24 h after the seeding. Although the metabolic activity significantly decreased in the samples with the most concentrated platelets (PCL/P1-P3) on days 3 and 7, afterward it started to increase again. The highest metabolic activity was seen in the PCL/P2 scaffold on day 14. The samples with lower platelet number and the control PCL sample showed stable or slightly increased metabolic activity during the whole experiment.

Cells in the samples with a higher concentration of platelets (PCL/P1–P3) started to proliferate noticeably from day 3 to day 7. The fast increase in the cell numbers resulted in a decrease in the cell metabolic activity, when related to the DNA content. The cell growth started to slow down in these samples on day 10, which corresponded with an increase in metabolic activity. The decrease in cell proliferation was probably caused by the depletion of nutrients, since the culture medium was not changed during the experiment. Fast growing cells on the scaffolds with higher concentrations of platelets (PCL/P1–P3) exhausted the nutrients faster than the cells on the scaffolds with lower concentrations of platelets or no platelets (PCL/P4, PCL/P5 and PCL).

Osteogenic activity of MG-63 cells

The activity of ALP and immunodetection of OCN were used to measure the stimulation of osteogenic differentiation by platelets. Figure 3D shows that the higher concentrations of platelets increased the ALP activity. PCL/P1 showed the highest ALP activity compared to all the other samples on days 7 and 14. Lower ALP activity was detected in the PCL/

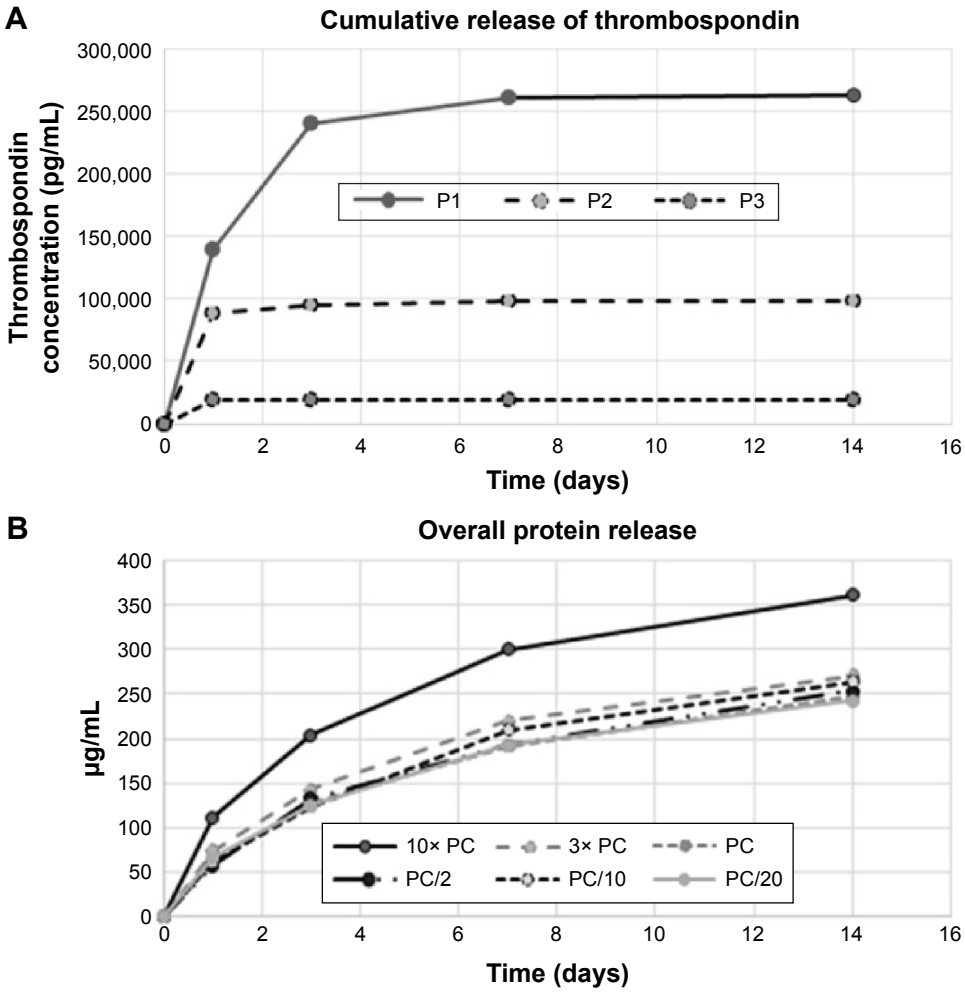

Figure 2 Release kinetics of protein from platelets.
Notes: Thrombospondin was used as a model protein to detect the release kinetics from platelets (**A**). Release of thrombospondin was dose dependent and was detectable only for higher concentrations of platelets (P1–P3). Samples with lower platelet concentrations were below the ELISA kit detection limit (P4 and P5). Total protein release was measured using fluorescence probe (**B**). Dependence on platelet concentrations was shown only for the highest concentration (10× PC = P1). In lower concentrations, results were influenced by the presence of plasma proteins.
Abbreviations: P, platelets; ELISA, enzyme-linked immunosorbent assay; PC, physiological concentration.

P2 sample, although the ALP activity was higher than in all the samples with lower platelet concentration or no platelets (PCL/P3–P4, PCL).

Visualization of OCN via confocal microscopy did not confirm the osteogenic stimulation of platelets. There were only small, sporadic islands of OCN. The largest amount of OCN was visible on the PCL/P1 and PCL/P2 scaffolds, respectively, on day 14 (data not shown).

Morphology of cells in samples analyzed by microscopy

The morphology and spreading of the cells on the scaffolds were visualized using both confocal microscope and SEM. The cells on the scaffolds were visualized using DiOC6 (internal cell membranes, green color) and PI (cell nuclei, red color) staining (Figure 4). The confocal microscopy showed good adhesion of cells to the PCL fibers. Cells adhered similarly on all the tested scaffolds. Besides the cells, adhered platelets were visible on day 1. The cells on the scaffolds were well spread, and during the culture their number was rising. The highest number of cells was visible on day 7. The microscope confirmed the trend from MTS and Picogreen assay, where cells showed higher proliferation with the increase in platelet concentration. The highest number of cells was detected in the PCL/P1 sample and the lowest in PCL/P5 and control PCL sample. On day 14, the cell number was decreasing. The numbers of cells on the scaffolds with a low concentration of platelets (PCL/P3, PCL/P4) and control sample (PCL) were constant during the experiment. The results correlate well with the data from DNA analysis. The results of SEM analysis confirmed that the cells were adhered to the fibers and showed a well-spread morphology.

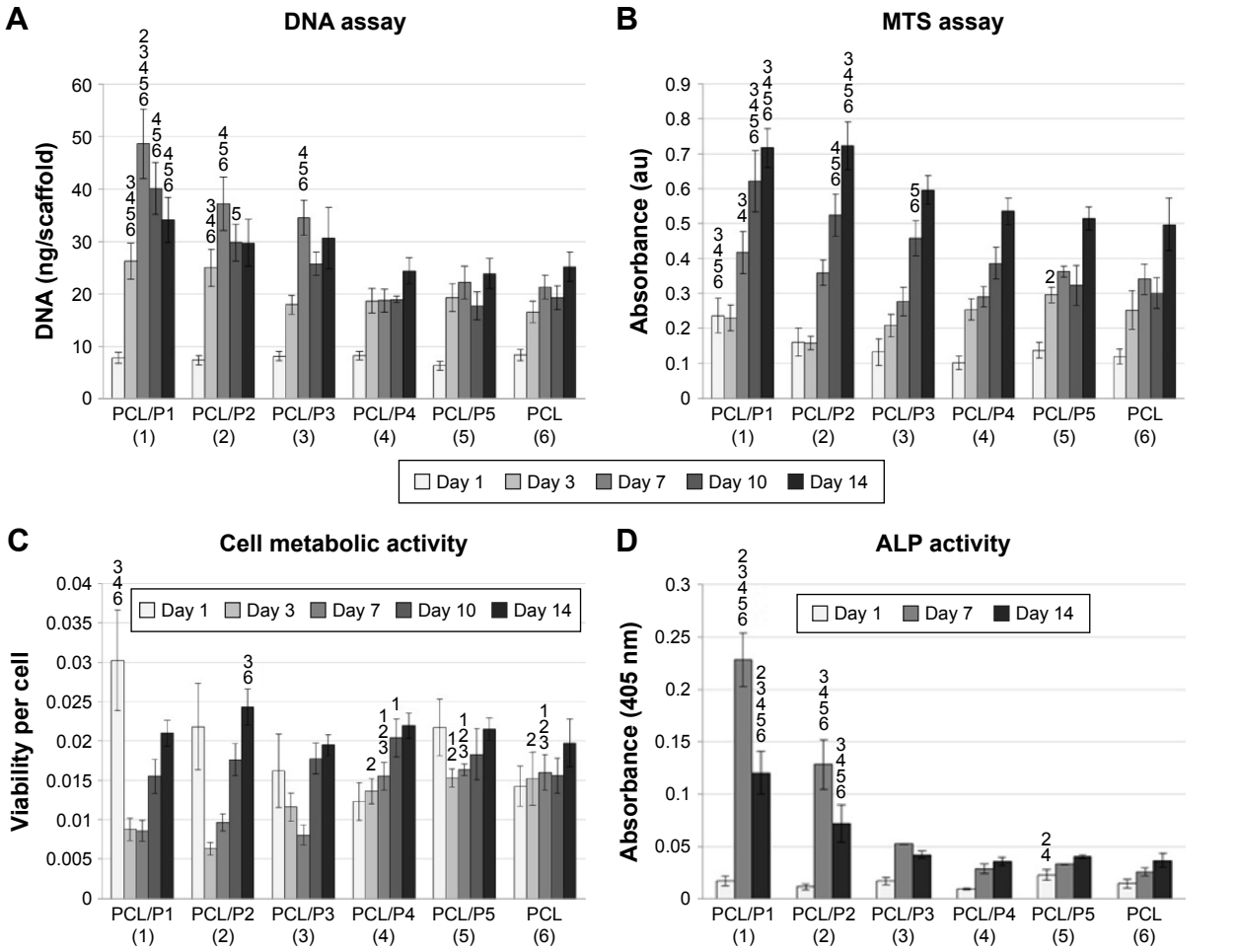

Figure 3 MG-63 cell proliferation, metabolic activity and ALP activity.
Notes: Cell proliferation was measured using quantification of DNA (**A**). Cell metabolic activity was measured using MTS assay (**B**). Both cell proliferation and metabolic activity were highest in samples with the highest platelet concentrations (PCL/P1 and PCL/P2). Metabolic activity was subsequently related to the DNA content (**C**). ALP activity was highest in samples with the highest platelet concentrations (PCL/P1 and PCL/P2; **D**). The numbers above the columns in the graphs represent the numbers of the samples (corresponding to numbers in parentheses on the *x*-axis) to show statistically significant differences.
Abbreviations: PCL, poly-ε-caprolactone; P, platelets; ALP, alkaline phosphatase.

In addition, due to higher pore size compared to electrospun scaffolds,[16] the cells penetrated into the scaffold. In all groups, the penetration depth was ~80–90 μm, and only on the PCL/P1 group, the penetration was deeper (120 μm; Figure 5).

Samples were also visualized using an SEM to detect cell morphology and adhesion in more detail (Figure 6). Cells adhered well on polymeric fibers and were well spread. No difference was seen between the groups.

Discussion

Bone and cartilage defects are among the most prevalent reasons for disability in the population worldwide. Due to the 3D nature of bone and cartilage tissue, the scaffolds for their regeneration should support cell growth in all 3 dimensions. Three-dimensional scaffolding systems are in high demand in tissue engineering. In order to address this challenge, a system with high porosity and open pores is needed. Different strategies have been used to prepare fibrous scaffolds for tissue engineering applications. Currently, the most popular method is electrospinning. A classical electrospinning device layout gives rise to sheet-like layers of fibers. These layers have large porosity and a big surface to volume ratio, with excellent adhesive capacity. A disadvantage of the electrospun layers is a 2D-like structure with small pores. Most tissue engineering applications demand 3D-structured scaffolds with open pores to enable cell infiltration. Different strategies such as special collectors[17] and salt leaching[18] were used to enhance the pore size and thickness of nanofibrous layers. Currently, alternative methods to prepare nano- and microfibers, such as melt-blown or centrifugal spinning, are being tested for tissue engineering applications. In our previous work, we have shown that PCL scaffolds prepared by centrifugal spinning technology, unlike electrospinning

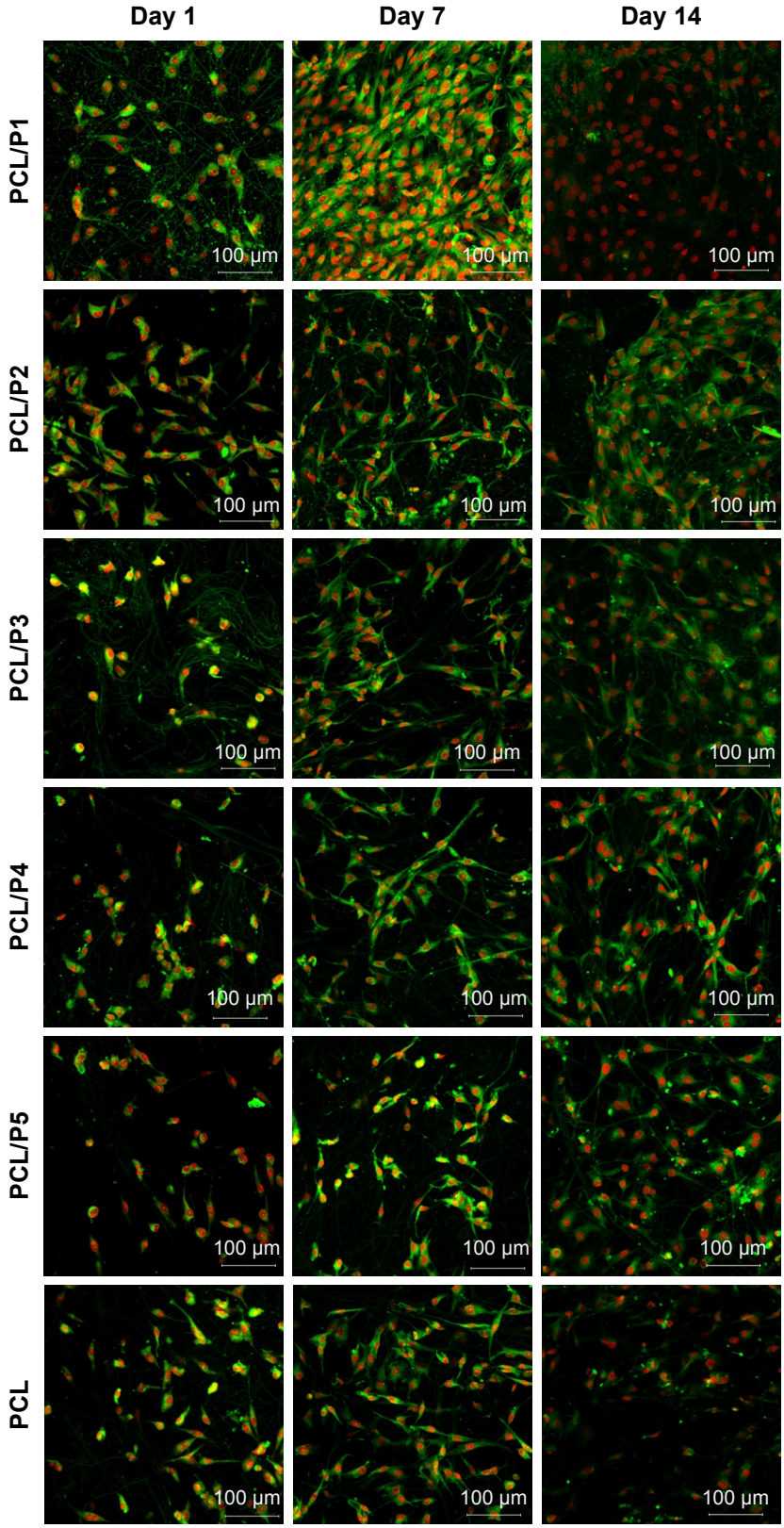

Figure 4 Visualization of MG-63 cells on scaffolds prepared using centrifugal spinning.
Notes: Cells were stained using DiOC6 (internal cell membranes, green color) and propidium iodide (cell nuclei, red color) and visualized using a confocal microscope. Cells adhered similarly on all the tested scaffolds. The highest number of cells was visible on the PCL/P1 on day 7. On day 14, the cell number was decreasing. The numbers of cells on the scaffolds with low concentrations of platelets (PCL/P3, PCL/P4) and control sample (PCL) were constant during the experiment. The results correspond well with the data from DNA analysis.
Abbreviations: DiOC6, 3,3′-diethyloxacarbocyanine iodide; PCL, poly-ε-caprolactone; P, platelets.

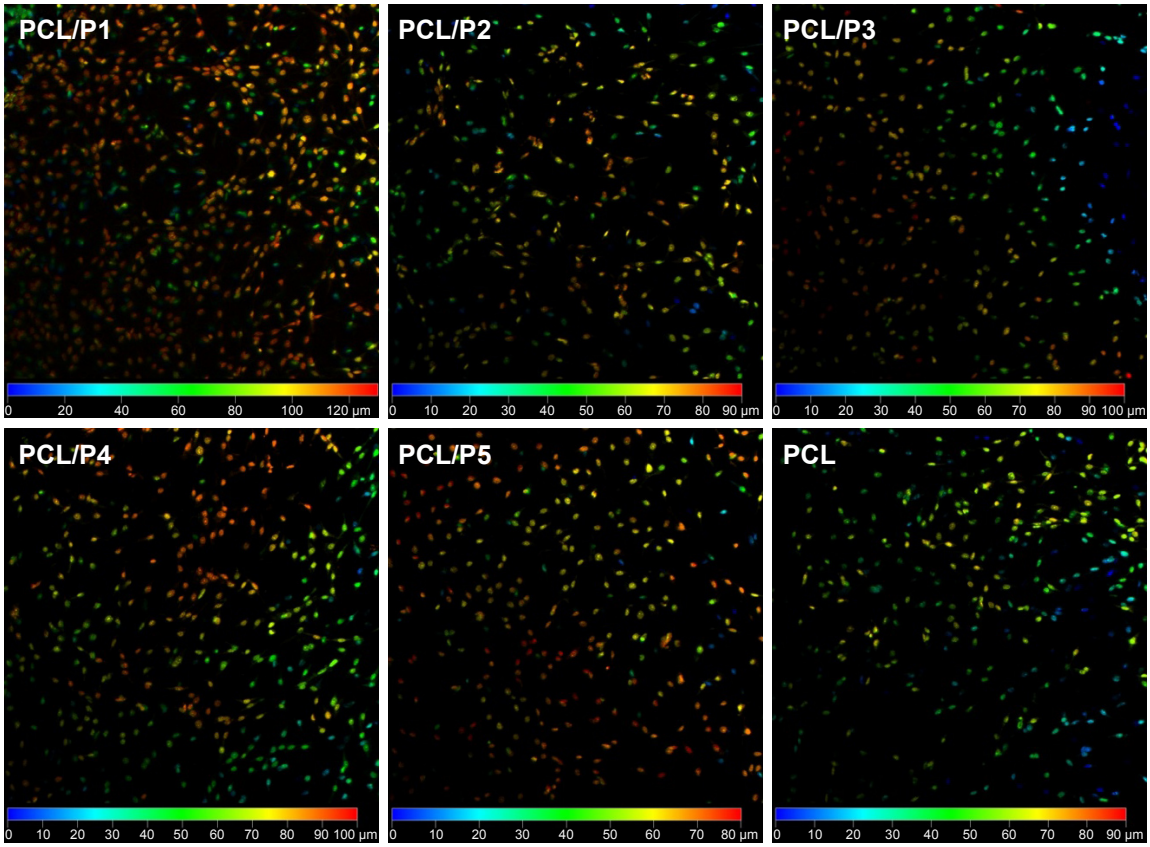

Figure 5 Cell infiltration into the scaffolds.
Notes: Cell nuclei visualized using confocal microscope were labeled based on their position inside fibrous scaffolds. The color scale shows cells in different depths of the scaffold. Cell infiltration was similar on all the scaffolds (80–90 µm) except for the PCL/P1, where cells penetrated to the depth of 120 µm.
Abbreviations: PCL, poly-ε-caprolactone; P, platelets.

scaffolds, show morphology favoring cell penetration.[16] The results of the current study confirmed that the cells were able to penetrate as deep as 120 µm in the PCL/P1 sample.

Stimulation of cell migration inside the scaffold and their differentiation toward the required cell type is essential for successful tissue regeneration. Only correctly differentiated cells can produce proteins of ECM of the right composition and ratio for the particular tissue. The cellular differentiation is regulated by numerous stimuli including the mechanical properties of the surrounding tissue, tension of oxygen, small molecular weight signaling molecules and protein-based morphogens (ie, growth factors). The differentiation process is an interplay of these stimuli. A wide range of bioactive stimulating molecules has been studied for bone tissue engineering.

Bone tissue healing upon injury is a complex process involving a number of cytokines, chemokines and growth factors. The early phases of bone regeneration are associated with hemostasis and inflammation in the fracture site. Platelets play a pivotal role in these early phases of healing. IL-1[19] and IL-6[20] as pro-inflammatory cytokines play a role in macrophage activation. IL-17 was shown to be one of the key regulators in the early phases of bone healing via osteoblast maturation.[21,22] IL-17 was found in high levels in platelets. In addition, IL-1, TNF-α, SDF-1 and GCSF stimulate mesenchymal progenitor cell activation.[23] The multiplex analysis confirmed that TNF-α, IL-1ra and GCSF were present in the platelets adhered to the proposed scaffold. Delivery of these stimuli may help initiate the regeneration process. In later phases, growth factors play a pivotal role in the regulation of tissue regeneration. The most prominent growth factors efficient in the early phases of bone healing include SDF-1α recruiting the progenitor cells to the site of injury, bFGF promoting proliferation of progenitor cells, IGF-I acting as an antiapoptotic and pro-osteogenic factor and TGF-β stimulating osteogenic differentiation. In the middle and late phases, the roles of BMP-2, BMP-7 and IGF-I become the most dominant.[23] The presence of PDGF was also observed to have a positive effect on bone repair.[24] Bone tissue neovascularization is regulated by VEGF and is essential for bone tissue integrity restoration. In order to develop a successful scaffold, the system should deliver these growth factors.

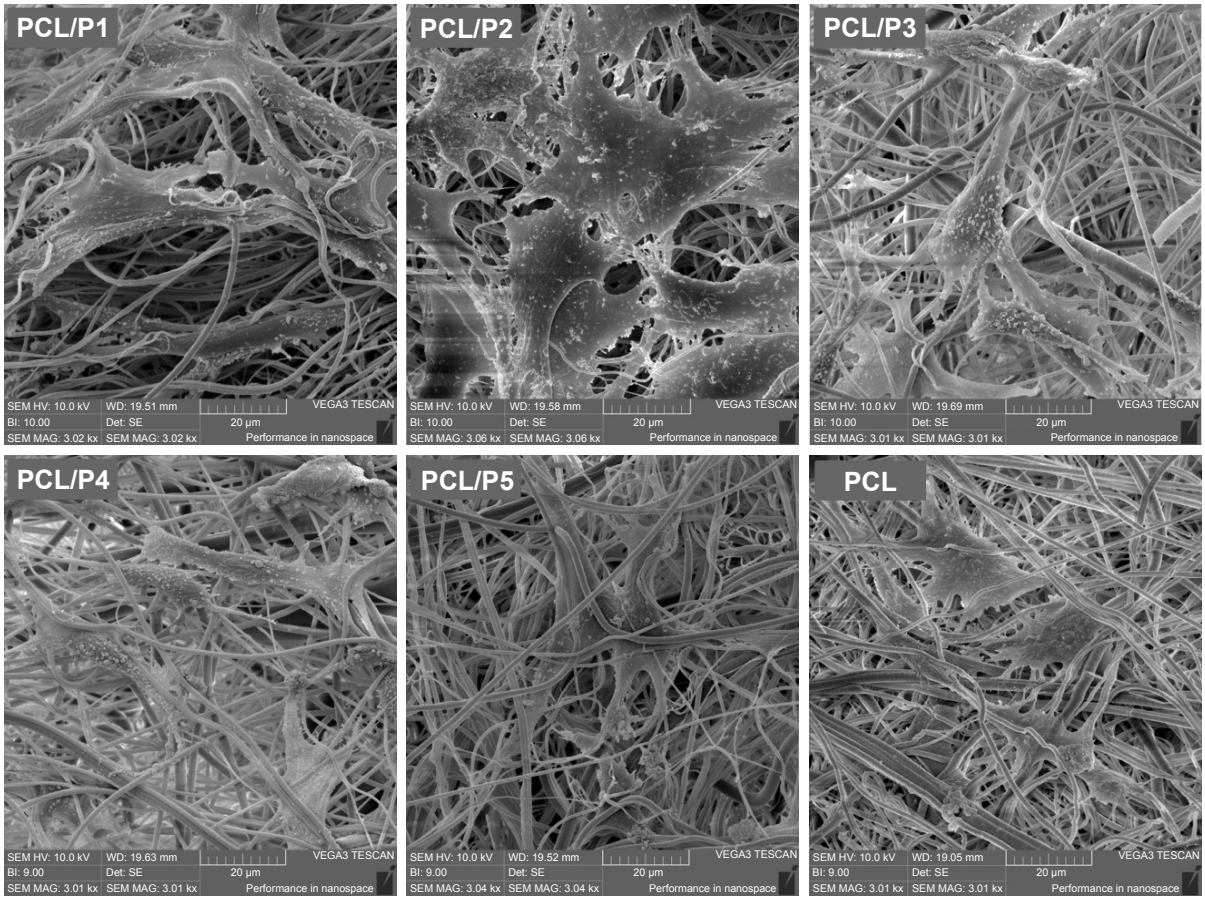

Figure 6 Visualization of the adhered cells using SEM.
Notes: Cells were uniformly distributed and well spread on the scaffolds. A similar picture was seen on all the samples. Day 7, magnification 3,000×.
Abbreviations: SEM, scanning electron microscope; PCL, poly-ε-caprolactone; P, platelets.

The multiplex assay identified the presence of PDGF-bb, VEGF, bFGF and other growth factors. Analysis by ELISA confirmed the presence of TGF-β, IGF-I and EGF. However, the other active molecules identified by multiplex assay also have relevance for bone tissue engineering. RANTES was identified in high concentration and was shown to play a role in the osteogenic differentiation of MSCs.[25]

Besides a stimulatory role, the released molecules may inhibit the progress of the bone healing process. In biomaterials research, TNF-α and IL-1 are the best known mediators of the foreign body reaction. Lange et al[19] observed the positive effect of IL-1β on the proliferation of osteoblasts and the negative effect on the proliferation and differentiation of MSCs. Similarly, TNF-α was shown to inhibit the progress of bone healing by inducing osteoblast and chondrocyte apoptosis.[26,27] However, some reports show that some level of TNF-α signalizing is necessary for bone resorption during the repair process.[28] Thrombospondin is one of the most abundant platelet proteins. Thrombospondin is an inhibitor of vascularization, and several studies also showed its negative influence on bone healing. Hsu et al[29] showed in his study that thrombospondin (TSHB) negatively influences the proliferation of different cell types (periodontal ligament cells [PDL], osteoblasts and endothelial cells) in concentrations >2.5 µg/mL. The mean level of thrombospondin in our samples was ~94 ng/mL, and the inhibitory effect therefore may be lower.[29]

Nevertheless, the current study employed multiplexed immunoassays and ELISA, which have limited capacity and sensitivity. Therefore, we have identified and quantified only part of the proteins present in the platelets. A complex proteomic analysis showed >500 proteins in platelet proteome.[30] A study of thrombin-induced release showed >90 proteins in platelet releasate.[31] In addition, the platelet protein content highly fluctuates in donors depending on gender, age and physiological state.[30] In a recent study, Mussano et al[32] performed a similar X-MAP multiplex assay on male and female platelets. The result showed differences with our results. In our case, IL-17, VEGF and PDGF-bb concentration was higher and INF-γ concentration was lower compared to the described study. In addition, the multiplexed assay

was more sensitive than standard ELISA. For instance, bFGF in our sample was not measurable using the standard ELISA protocol.

Platelets are, for their regenerative potential, currently often used in regenerative medicine.[33] The key strategies for platelet preparation include buffy coat and apheresis methods.[34–37] The buffy coat method, which was used in this manuscript, is based on centrifugation of the whole blood to separate platelets, leukocytes, erythrocytes and plasma. The excess erythrocytes and leukocytes are removed via specific filtration. The key advantage of the buffy coat method is the possibility to prepare large batches of platelets from mixed donors. On the other hand, apheresis is based on online platelet separation from a single donor. Although the platelet concentrates are less contaminated by leukocytes and erythrocytes, the method is rather time-consuming and requires complex apparatuses. In clinical practice, the platelets for chirurgical application could be isolated on site by specific concentrators. The systems are based on diverse modifications of the buffy coat method and commercialized under trade names such as Plateltex, SmartPReP, PCCS and Magellan.[34,35] From application point of view, the commercial methods enable isolation of autologous platelets. The key advantages of autologous platelets are elimination of disease transmission, possible immune reaction and high compatibility with the patient. On the other hand, allogenic platelet formulations enable rapid donation even to patients in life-threatening states. The allogenic preparations based on buffy coat also enable elimination of donor-to-donor variations by preparing mixed platelet isolates from multiple donors. The importance of the problem was highlighted by Lohmann et al,[38] who observed relationship between patient age and proliferation of MSCs.

The isolated platelet formulation highly differs in its properties. According to Dohan Ehrenfest et al,[34,35] the platelet formulations may be divided into pure PRP (P-PRP), leukocyte and PRP (L-PRP), pure platelet-rich fibrin (P-PRF) and leukocyte and platelet-rich fibrin (L-PRF). The differences are the presence of leukocytes and activation state of platelets. In the current manuscript, we have used P-PRP for adhesion to fibers. On the other hand, activated platelets provide interesting properties for tissue engineering applications.

Platelets, when they are activated, create fibrin net and release various growth factors and cytokines. This natural process is used as a scaffolding material. To date, platelets have showed great promise mainly in the field of maxillofacial bone reconstruction. The fibrin gels made completely of platelets show high cell adhesion, proliferation[39] and bone repair.[40,41] However, the fibrin gel formed by activation of platelets is stable only for a few days. Rapid degradation of fibrin has been studied in various studies.[42–44] Bardsley et al[43] showed in his study high initial in vitro degradation of fibrin gel between 0 and 5 days. It was shown that the degradation rate can be slowed down by combining with hyaluronic acid and laminin[42] or polyethylenglycol.[45] While fibrin-only gel totally degrades after 14 days of cultivation, PEGylated fibrin stayed intact. In addition, the pore size of fibrin gel is lower due to the packed morphology of fibrin fibers.[46] Therefore, the cell penetration is connected with fibrin gel degradation.[43] On the other hand, PCL is a biocompatible and biodegradable polymer, which degrades after several months.[47] The material proposed in this study shows longer stability and is more suitable for reconstruction of critical defects, which need prolonged stabilization of the scaffolds. Slow degradation enables cells to synthesize the ECM and gradually form new tissue. Especially, the bone regeneration in critical bone defects (ie, long bones and large extractions) takes several months. In such indications, the fibrin gel cannot show sufficient stability. The material in the present study showed that the adhered platelets were able to form fibrin net on the fibers and showed improved initial cellular adhesion of model cells compared to the pure PCL scaffold. In addition, the centrifugal spinning technology enables formation of large fluffy fibrous scaffolds with interconnected pore morphology enabling cell penetration. From the drug release point of view, the addition of platelets is key for the delivery of active molecules. The effect of growth factor delivery improved the scaffold colonization both in vitro[48] and in vivo.[10]

The importance of the adhesion of the platelets to the surface of fibers is mainly in their immobilization. The results of SEM and the release study showed that platelets delivered active molecules for several days. The active molecules identified in platelets may therefore improve tissue regeneration. For comparison with fibrin gel, a study by Dohan Ehrenfest et al[49] showed that platelet fibrin gel released growth factors up to 7 days.The present study showed that platelets adhered on fibers release growth factors even after the 7th day. We believe that this phenomenon was observed because of fibrin net degradation upon colonization of deeper scaffold layer and liberation of the attached growth factors. The mechanism behind the release in this system may be connected with 2 phenomena. The intact platelets were shown on the scaffold even after 14 days of incubation, which indicates that they were viable and able to secrete their cargo. The second mechanism for sustained release is connected with

degradation of the fibrin net. The fibrin net binds growth factors and through degradation the attached proteins are liberated. After 14 days, both the decreased number of intact platelets on the scaffold and the degraded fibrin net were observed. Therefore, the release by both mechanisms was attenuated. The functionalization of fibrous scaffolds may be performed via encapsulation or surface binding of platelet derivatives. Only a limited number of studies report using scaffolds prepared via centrifugal electrospinning as a drug delivery system. In a study by Mary et al,[50] tetracycline-loaded PCL-blended polyvinylpyrrolidone (PVP) fibers were used as a drug delivery vehicle. The prepared fibers showed rapid drug release followed by a sustained release and good antimicrobial activity against pathogenic bacteria, which are commonly found in dermal infections. In the current study, we focused on the delivery of regeneration promoting substances. The platelets were adhered to the surface of fibers and provided bioactive molecules. The results of metabolic activity and proliferation assays showed that the factors stimulated MG-63 cell proliferation. The cell proliferation was dose dependent, and with an increase in the platelet concentration the cells showed a higher proliferation rate and increased metabolic activity.

MG-63 is a cell line derived from human osteosarcoma. These cells are frequently used in tissue engineering studies to study scaffold biocompatibility and bone tissue formation.[51–55] On the other hand, differences between osteosarcoma lines and primary osteoblast cells have been published.[56,57] Main differences have been found in proliferation kinetics, cell morphology and synthesis of ECM proteins. For this reason, further experiments using primary osteoblast cells or MSCs will be necessary to confirm the positive effect of the fibrous scaffold–platelet system on specific cell infiltration and osteogenic differentiation.

The results are similar to those of Diaz-Gomez et al,[15] who observed that adhesion of PRP to PCL nanofibers promotes proliferation of MSCs. Similarly, Buzgo et al[58] found that embedded alpha granules were able to stimulate the chondrogenic differentiation of MSCs. In addition, the stimulatory role of platelets in bone regeneration was confirmed by Anjana et al,[59] Getgood et al[60] and Prosecká et al.[10]

The additional advantage of surface functionalization by platelets, when compared to encapsulation, is the much simpler scaffold preparation. The system enables modification in the outpatient clinic and solves the problems associated with the long-term storage of the scaffolds. In addition, the utilized platelets may be autologous, thus minimizing the risks associated with the use of allogenous platelets, such as disease transmission and immune reaction. In the present study, the performance of the system was evaluated in the model of MG-63 osteoblasts. The samples functionalized by platelets showed improved proliferation, metabolic activity and ALP activity. Cell penetration is essential for bone tissue engineering scaffolds. Prosecká et al[10] recently produced a collagen/hydroxyapatite scaffold prepared using the freeze drying process. However, the foam scaffolds showed problems with pore interconnection. In the case of the fibrous scaffolds produced by centrifugal spinning, the pores are highly interconnected and allow efficient cell migration. Confocal microscopy showed that due to the 3D structure of the fibrous matrix the cells were able to penetrate deep into the scaffold. The biological properties of the system described in this work are therefore a simple and clinically translatable system for bone tissue engineering.

Conclusion

Centrifugal electrospinning is a simple method for producing 3D fibrous scaffolds. However, the complex osteogenic regeneration process requires stimulation by active molecules. Herein, we have introduced a simple composite scaffold based on platelet adhesion to PCL 3D fibers. The platelets are a source of growth factors and cytokines active in tissue repair. The multiplexed immunoassay showed the presence of a high concentration of IL-17, RANTES, PDGF-bb, TGF-β and other molecules active in the bone healing process. The immobilization on a fibrous scaffold prolonged the bioavailability of these active molecules. The biological evaluation in the MG-63 model showed improved metabolic activity, proliferation and ALP activity compared to nonfunctionalized fibrous scaffold. In addition, the response of cells was dose dependent with improved biocompatibility with increasing platelet concentration. The results demonstrated the suitability of the system for bone tissue engineering.

Acknowledgments

This research was supported by the Czech Science Foundation Grant No 15-15697S and the Ministry of Education, Youth and Sports of the Czech Republic (Research Programs NPU I:LO1508).

Disclosure

The authors report no conflicts of interest in this work.

References

1. Sill TJ, von Recum HA. Electrospinning: applications in drug delivery and tissue engineering. *Biomaterials*. 2008;29(13):1989–2006.

2. Agarwal S, Wendorff JH, Greiner A. Use of electrospinning technique for biomedical applications. *Polymer*. 2008;49(26):5603–5621.
3. Zhou F-L, Gong R-H, Porat I. Mass production of nanofibre assemblies by electrostatic spinning. *Polym Int*. 2009;58(4):331–342.
4. Zander NE. Formation of melt and solution spun polycaprolactone fibers by centrifugal spinning. *J Appl Polym Sci*. 2015;132(2).
5. Loordhuswamy AM, Krishnaswamy VR, Korrapati PS, Thinakaran S, Rengaswami GDV. Fabrication of highly aligned fibrous scaffolds for tissue regeneration by centrifugal spinning technology. *Mater Sci Eng C Mater Biol Appl*. 2014;42:799–807.
6. Rampichova M, Buzgo M, Chvojka J, Prosecka E, Kofronova O, Amler E. Cell penetration to nanofibrous scaffolds: Forcespinning®, an alternative approach for fabricating 3D nanofibers. *Cell Adh Migr*. 2014;8(1):36–41.
7. Ren L, Pandit V, Elkin J, Denman T, Cooper JA, Kotha SP. Large-scale and highly efficient synthesis of micro- and nano-fibers with controlled fiber morphology by centrifugal jet spinning for tissue regeneration. *Nanoscale*. 2013;5(6):2337–2345.
8. Wang L, Shi J, Liu L, Secret E, Chen Y. Fabrication of polymer fiber scaffolds by centrifugal spinning for cell culture studies. *Microelectron Eng*. 2011;88(8):1718–1721.
9. Blair P, Flaumenhaft R. Platelet alpha-granules: basic biology and clinical correlates. *Blood Rev*. 2009;23(4):177–189.
10. Prosecká E, Rampichova M, Litvinec A, et al. Collagen/hydroxyapatite scaffold enriched with polycaprolactone nanofibers, thrombocyte-rich solution and mesenchymal stem cells promotes regeneration in large bone defect in vivo. *J Biomed Mater Res A*. 2015;103(2):671–682.
11. Jakubova R, Mickova A, Buzgo M, et al. Immobilization of thrombocytes on PCL nanofibres enhances chondrocyte proliferation in vitro. *Cell Prolif*. 2011;44(2):183–191.
12. Wang X, Qiu Y, Triffitt J, Carr A, Xia Z, Sabokbar A. Proliferation and differentiation of human tenocytes in response to platelet rich plasma: an in vitro and in vivo study. *J Orthop Res*. 2012;30(6):982–990.
13. Plencner M, Prosecka E, Rampichova M, et al. Significant improvement of biocompatibility of polypropylene mesh for incisional hernia repair by using poly-epsilon-caprolactone nanofibers functionalized with thrombocyte-rich solution. *Int J Nanomedicine*. 2015;10:2635–2646.
14. Lacci KM, Dardik A. Platelet-Rich plasma: support for its use in wound healing. *Yale J Biol Med*. 2010;83(1):1–9.
15. Diaz-Gomez L, Alvarez-Lorenzo C, Concheiro A, et al. Biodegradable electrospun nanofibers coated with platelet-rich plasma for cell adhesion and proliferation. *Mater Sci Eng C Mater Biol Appl*. 2014;40:180–188.
16. Rampichova M, Buzgo M, Chvojka J, Prosecka E, Kofronova O, Amler E. Cell penetration to nanofibrous scaffolds. *Cell Adh Migr*. 2014;8(1):36–41.
17. Rampichova M, Chvojka J, Buzgo M, et al. Elastic three-dimensional poly (epsilon-caprolactone) nanofibre scaffold enhances migration, proliferation and osteogenic differentiation of mesenchymal stem cells. *Cell Prolif*. 2013;46(1):23–37.
18. Rnjak-Kovacina J, Weiss AS. Increasing the pore size of electrospun scaffolds. *Tissue Eng Part B Rev*. 2011;17(5):365–372.
19. Lange J, Sapozhnikova A, Lu CY, et al. Action of IL-1 beta during fracture healing. *J Orthop Res*. 2010;28(6):778–784.
20. Yang X, Ricciardi BF, Hernandez-Soria A, Shi Y, Camacho NP, Bostrom MPG. Callus mineralization and maturation are delayed during fracture healing in interleukin-6 knockout mice. *Bone*. 2007;41(6):928–936.
21. Nam D, Mau E, Wang YF, et al. T-lymphocytes enable osteoblast maturation via IL-17F during the early phase of fracture repair. *PLoS One*. 2012;7(6):e40044.
22. Ono T, Okamoto K, Nakashima T, et al. IL-17-producing gamma delta T cells enhance bone regeneration. *Nat Commun*. 2016;7:10928.
23. Mehta M, Schmidt-Bleek K, Duda GN, Mooney DJ. Biomaterial delivery of morphogens to mimic the natural healing cascade in bone. *Adv Drug Deliv Rev*. 2012;64(12):1257–1276.
24. Santo VE, Frias AM, Carida M, et al. Carrageenan-based hydrogels for the controlled delivery of PDGF-BB in bone tissue engineering applications. *Biomacromolecules*. 2009;10(6):1392–1401.
25. Liu YC, Kao YT, Huang WK, et al. CCL5/RANTES is important for inducing osteogenesis of human mesenchymal stem cells and is regulated by dexamethasone. *BioSci Trends*. 2014;8(3):138–143.
26. Zhou FH, Foster BK, Zhou XF, Cowin AJ, Xian CJ. TNF-alpha mediates p38 MAP kinase activation and negatively regulates bone formation at the injured growth plate in rats. *J Bone Miner Res*. 2006;21(7):1075–1088.
27. Sun MQ, Yang JL, Wang JZ, et al. TNF-alpha is upregulated in T2DM patients with fracture and promotes the apoptosis of osteoblast cells in vitro in the presence of high glucose. *Cytokine*. 2016;80:35–42.
28. Gerstenfeld LC, Cho TJ, Kon T, et al. Impaired intramembranous bone formation during bone repair in the absence of tumor necrosis factor-alpha signaling. *Cells Tissues Organs*. 2001;169(3):285–294.
29. Hsu CW, Yuan K, Tseng CC. The negative effect of platelet-rich plasma on the growth of human cells is associated with secreted thrombospondin-1. *Oral Surg Oral Med Oral Pathol Oral Radiol Endod*. 2009;107(2):185–192.
30. Dzieciatkowska M, D'Alessandro A, Burke TA, et al. Proteomics of apheresis platelet supernatants during routine storage: gender-related differences. *J Proteomics*. 2015;112:190–209.
31. van Holten TC, Bleijerveld OB, Wijten P, et al. Quantitative proteomics analysis reveals similar release profiles following specific PAR-1 or PAR-4 stimulation of platelets. *Cardiovasc Res*. 2014;103(1):140–146.
32. Mussano F, Genova T, Munaron L, Petrillo S, Erovigni F, Carossa S. Cytokine, chemokine, and growth factor profile of platelet-rich plasma. *Platelets*. 2016;27(5):467–471.
33. Kon E, Filardo G, Di Martino A, Marcacci M. Platelet-rich plasma (PRP) to treat sports injuries: evidence to support its use. *Knee Surg Sports Traumatol Arthrosc*. 2011;19(4):516–527.
34. Dohan Ehrenfest DM, Andia I, Zumstein MA, Zhang C-Q, Pinto NR, Bielecki T. Classification of platelet concentrates (Platelet-Rich Plasma-PRP, Platelet-Rich Fibrin-PRF) for topical and infiltrative use in orthopedic and sports medicine: current consensus, clinical implications and perspectives. *Muscles Ligaments Tendons J*. 2014;4(1):3–9.
35. Dohan Ehrenfest DM, Rasmusson L, Albrektsson T. Classification of platelet concentrates: from pure platelet-rich plasma (P-PRP) to leucocyte- and platelet-rich fibrin (L-PRF). *Trends Biotechnol*. 2009;27(3):158–167.
36. Gulliksson H. Platelets from platelet-rich-plasma versus buffy-coat-derived platelets: what is the difference? *Rev Bras Hematol Hemoter*. 2012;34(2):76–77.
37. Bock M, Rahrig S, Kunz D, Lutze G, Heim MU. Platelet concentrates derived from buffy coat and apheresis: biochemical and functional differences. *Transfus Med*. 2002;12(5):317–324.
38. Lohmann M, Walenda G, Hemeda H, et al. Donor age of human platelet lysate affects proliferation and differentiation of mesenchymal stem cells. *PLoS One*. 2012;7(5):e37839.
39. Dohan Ehrenfest DM, Doglioli P, de Peppo GM, Del Corso M, Charrier JB. Choukroun's platelet-rich fibrin (PRF) stimulates in vitro proliferation and differentiation of human oral bone mesenchymal stem cell in a dose-dependent way. *Arch Oral Biol*. 2010;55(3):185–194.
40. Durmuslar MC, Balli U, Ongoz Dede F, et al. Evaluation of the effects of platelet-rich fibrin on bone regeneration in diabetic rabbits. *J Craniomaxillofac Surg*. 2016;44(2):126–133.
41. Wang Z, Hu H, Li Z, et al. Sheet of osteoblastic cells combined with platelet-rich fibrin improves the formation of bone in critical-size calvarial defects in rabbits. *Br J Oral Maxillofac Surg*. 2016;54(3):316–321.
42. Arulmoli J, Wright HJ, Phan DT, et al. Combination scaffolds of salmon fibrin, hyaluronic acid, and laminin for human neural stem cell and vascular tissue engineering. *Acta Biomater*. 2016;43:122–138.

43. Bardsley K, Wimpenny I, Wechsler R, Shachaf Y, Yang Y, El Haj AJ. Defining a turnover index for the correlation of biomaterial degradation and cell based extracellular matrix synthesis using fluorescent tagging techniques. *Acta Biomater*. 2016;45:133–142.
44. Zhang Y, Heher P, Hilborn J, Redl H, Ossipov DA. Hyaluronic acid-fibrin interpenetrating double network hydrogel prepared in situ by orthogonal disulfide cross-linking reaction for biomedical applications. *Acta Biomater*. 2016;38:23–32.
45. Benavides OM, Quinn JP, Pok S, Petsche Connell J, Ruano R, Jacot JG. Capillary-like network formation by human amniotic fluid-derived stem cells within fibrin/poly(ethylene glycol) hydrogels. *Tissue Eng Part A*. 2015;21(7–8):1185–1194.
46. Sadeghi-Ataabadi M, Mostafavi-pour Z, Vojdani Z, Sani M, Latifi M, Talaei-Khozani T. Fabrication and characterization of platelet-rich plasma scaffolds for tissue engineering applications. *Mater Sci Eng C*. In press 2016.
47. Lam CX, Hutmacher DW, Schantz JT, Woodruff MA, Teoh SH. Evaluation of polycaprolactone scaffold degradation for 6 months in vitro and in vivo. *J Biomed Mater Res A*. 2009;90(3):906–919.
48. Santo VE, Duarte AR, Popa EG, Gomes ME, Mano JF, Reis RL. Enhancement of osteogenic differentiation of human adipose derived stem cells by the controlled release of platelet lysates from hybrid scaffolds produced by supercritical fluid foaming. *J Control Release*. 2012;162(1):19–27.
49. Dohan Ehrenfest DM, de Peppo GM, Doglioli P, Sammartino G. Slow release of growth factors and thrombospondin-1 in Choukroun's platelet-rich fibrin (PRF): a gold standard to achieve for all surgical platelet concentrates technologies. *Growth Factors*. 2009;27(1):63–69.
50. Mary LA, Senthilram T, Suganya S, et al. Centrifugal spun ultrafine fibrous web as a potential drug delivery vehicle. *Express Polym Lett*. 2013;7(3):238–248.
51. Cai Y, Yu J, Kundu SC, Yao J. Multifunctional nano-hydroxyapatite and alginate/gelatin based sticky gel composites for potential bone regeneration. *Mater Chem Phys*. 2016;181:227–233.
52. Hu J-X, Ran J-B, Chen S, Jiang P, Shen X-Y, Tong H. Carboxylated agarose (CA)-silk fibroin (SF) dual confluent matrices containing oriented hydroxyapatite (HA) crystals: biomimetic organic/inorganic composites for tibia repair. *Biomacromolecules*. 2016;17(7):2437–2447.
53. Chu S-F, Huang M-T, Ou K-L, et al. Enhanced biocompatible and hemocompatible nano/micro porous surface as a biological scaffold for functionalizational and biointegrated implants. *J Alloys Comp*. 2016;684:726–732.
54. Stevenson G, Rehman S, Draper E, Hernández-Nava E, Hunt J, Haycock JW. Combining 3D human in vitro methods for a 3Rs evaluation of novel titanium surfaces in orthopaedic applications. *Biotechnol Bioeng*. 2016;113(7):1586–1599.
55. Hejazi F, Mirzadeh H. Novel 3D scaffold with enhanced physical and cell response properties for bone tissue regeneration, fabricated by patterned electrospinning/electrospraying. *J Mater Sci Mater Med*. 2016;27(9):143.
56. Pautke C, Schieker M, Tischer T, et al. Characterization of osteosarcoma cell lines MG-63, Saos-2 and U-2 OS in comparison to human osteoblasts. *Anticancer Res*. 2004;24(6):3743–3748.
57. Bilbe G, Roberts E, Birch M, Evans DB. PCR phenotyping of cytokines, growth factors and their receptors and bone matrix proteins in human osteoblast-like cell lines. *Bone*. 1996;19(5):437–445.
58. Buzgo M, Jakubova R, Mickova A, et al. Time-regulated drug delivery system based on coaxially incorporated platelet alpha-granules for biomedical use. *Nanomedicine*. 2013;8(7):1137–1154.
59. Anjana J, Kuttappan S, Keyan KS, Nair MB. Evaluation of osteoinductive and endothelial differentiation potential of Platelet-Rich Plasma incorporated Gelatin-Nanohydroxyapatite Fibrous Matrix. *J Biomed Mater Res B Appl Biomater*. 2016;104(4):771–781.
60. Getgood A, Henson F, Brooks R, Fortier LA, Rushton N. Platelet-rich plasma activation in combination with biphasic osteochondral scaffolds-conditions for maximal growth factor production. *Knee Surg Sports Traumatol Arthrosc*. 2011;19(11):1942–1947.